

SPACE TIME MEASUREMENTS IN SPECIAL RELATIVITY

J.H.Field

Département de Physique Nucléaire et Corpusculaire Université de Genève . 24, quai
Ernest-Ansermet CH-1211 Genève 4.

Abstract

The conventional discussion of apparent distortions of space and time in Special Relativity (the Lorentz-Fitzgerald Contraction and Time Dilatation) is extended by considering observations of : (i) moving objects of limited lifetime in their own rest frame ('transient luminous objects') and (ii) a moving extended array of synchronised 'equivalent clocks' in a common inertial frame. Application of the Lorentz Transformation to (i) shows that such objects, viewed with coarse time resolution, appear to be *longer* in the direction of the relative velocity \vec{v} by a factor $1/\sqrt{1-(v/c)^2}$ (Space Dilatation) and to (ii) that the moving equivalent clock that appears at any fixed position in the rest frame of an inertial observer appears to be running *faster* than a similar clock at rest by the factor $1/\sqrt{1-(v/c)^2}$ (Time Contraction). The actual appearance of moving objects and clocks, taking into account light propagation time delays, as well as the effect of the Lorentz Transformation, is also discussed.

PACS 03.30+p

1 Introduction

In his 1905 paper on Special Relativity [1] Einstein showed that Time Dilatation (TD) and the Lorentz-Fitzgerald Contraction (LFC), which had previously been introduced in a somewhat ad hoc way into Classical Electrodynamics, are simple consequences of the Lorentz Transformation (LT), that is, of the geometry of space-time.

As an example of the LFC Einstein stated that a sphere moving with velocity v would, ‘viewed from the stationary system’, appear to be contracted by the factor $\sqrt{1 - (\frac{v}{c})^2}$ in its direction of motion where c is the velocity of light in free space. It was only pointed out some 54 years later that if ‘viewed’ was interpreted in the conventional sense of ‘as seen by the eye, or recorded on a photograph’ then the sphere does not at all appear to be contracted, but is still seen as a sphere with the same dimensions as a stationary one and at the same position [2, 3, 4] ! It was shown in general [3, 4] that transversely viewed moving objects subtending a small solid angle at the observer appear to be not distorted in shape or changed in size, but rather rotated, as compared to a similarly viewed and orientated object at rest. This apparent rotation is a consequence of three distinct physical effects:

- (i) The LFC.
- (ii) Optical Aberration.
- (iii) Different propagation times of photons emitted by different parts of the moving object.

The effect (ii) may be interpreted as the change in direction of photons, emitted by a moving source, due to the LT between the rest frames of the source and the stationary observer. Correcting for (ii) and (iii), the LFC can be deduced as a physical effect, if not directly observed. It was also pointed out by Weinstein [5] that if a single observer is close to a moving object then, because of the effect of light propagation time delays it will appear elongated if moving towards the observer and contracted (to an extent greater than the LFC) if moving away. Only an object moving strictly transversely to the line of sight of a close observer shows the LFC.

However, the LFC itself is a physical phenomenon similar in many ways to (iii) above. A photograph or the human eye record as a sharp image the photons incident on it at a fixed time. That is, the image corresponds to a projection at constant time in the frame S of observation. This implies that the photons constituting the image are emitted at different times from the different parts, along the line of sight, of an extended object. The LFC is similarly defined by a fixed time projection in the frame S . The LT then requires that the photons constituting the image of a moving object are also emitted at different times, in the rest frame S' of the object, from the different parts along its direction of motion. In the following S will, in general, denote the reference frame of a ‘stationary’ observer (space-time coordinates x, y, z, t) while S' refers to the rest frame of an object moving with uniform velocity v relative to S (space-time coordinates x', y', z', t').

The purpose of this paper is to point out that the $t = \text{constant}$ projection of the LFC

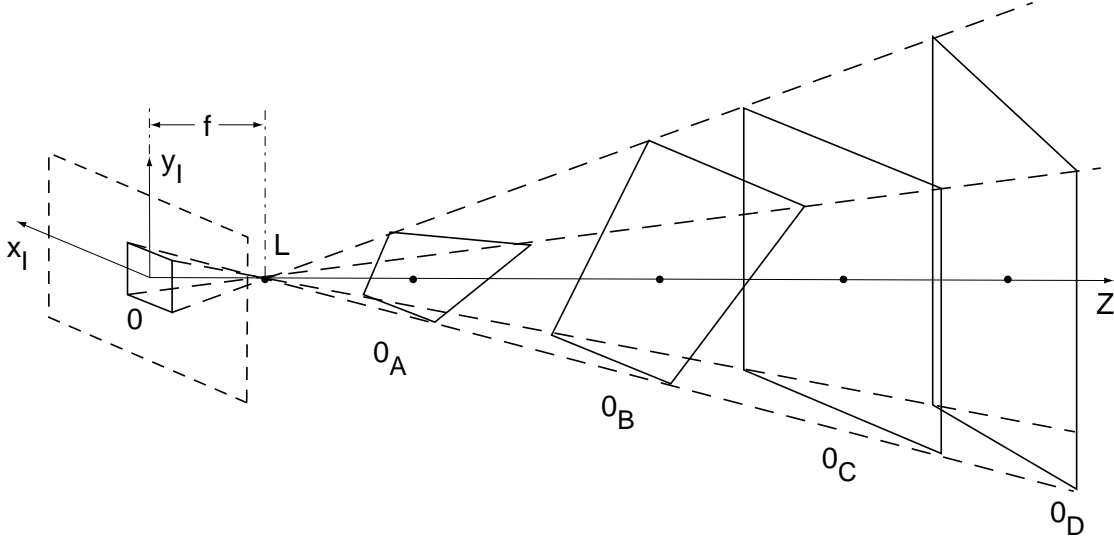
and the $x' = \text{constant}$ projection of TD are not the only physically distinct Space Time Measurements (STM) possible within Special Relativity. In fact, as will be demonstrated below, there are two others: Space Dilatation (SD), the $t' = \text{constant}$ projection and Time Contraction (TC), the $x = \text{constant}$ projection. The overall situation with respect to apparent distortions of space-time is thus symmetric with respect to space and time. The $t = \text{constant}$ projection of the LFC is the STM appropriate to the ‘moving bodies’ of Einstein’s original paper and to the photographic recording technique. This medium has no intrinsic time resolution and relies on that provided by a rapidly moving shutter to provide a clear image. The LFC ‘works’ as a well defined physical phenomenon because the ‘measuring rod’ or other physical object under observation has a lifetime that is long in comparison with the time interval required to make an observation, and so constitutes a continuous source of emitted or reflected photons, such that some are always available in the different space ($\Delta x'$) and time ($\Delta t'$) intervals in S' for every position of the rod corresponding to the time interval Δt around $t = \text{constant}$ in the observer’s frame S . If, however, the physical object of interest has internal motion (rotation, expansion or contraction) or is only illuminated, in its rest frame S' , during a short time interval, the above conditions, that assure that the $t = \text{constant}$ projection gives a well defined STM no longer apply. In the following, for brevity, all such objects of limited luminous lifetime in their own rest frame will be referred to as ‘Transient Luminous Objects’ or TLO. For such objects it is natural to define a length measurement by taking the $t' = \text{constant}$ projection in S' .

Space time measurements of such transient luminous objects are discussed below in Section 3. A simple conceptual camera of finite time resolution is considered. Practical examples are a flash camera or a TV raster. The camera is used to record Image Plane Coordinates (IPC) x_I, y_I, t_I in the observation frame S . To orient the discussion answers will be sought to the question: ‘What information about transient luminous objects (observed in general as a correlated ensemble of STM in the frame S) such as its distance, shape, orientation or lifetime can be derived *only* from measurements of the image plane coordinates? The case of stationary objects is first considered in Section 2, followed by the discussion of uniformly (transversely) moving objects in the following Section.

In Section 4 time measurements other than the conventional TD ($x' = \text{constant}$ projection) of Special Relativity are considered. The TD phenomenon refers only to a local clock, in the sense that its position in the frame S' is invariant (say at the spatial origin of coordinates). However the time recorded by any synchronised clock in the same inertial frame is, by definition, identical. Einstein used such an array of ‘equivalent clocks’ situated at different positions in the same inertial frame in his original discussion of the relativity of simultaneity [1]. The question addressed in Section 4 is: What will an observer in S see if he looks not only at a given local clock in S' , but also at other equivalent clocks at different positions in S' , in comparison to a standard clock at rest in his own frame? It is shown that such equivalent clocks may be seen to run slower than, or faster than, the TD prediction for a local clock. In particular they may even appear to *run faster than the standard clock*. This is an example of the Time Contraction effect mentioned above.

2 Space Time Measurements of Transient Luminous Objects at Rest

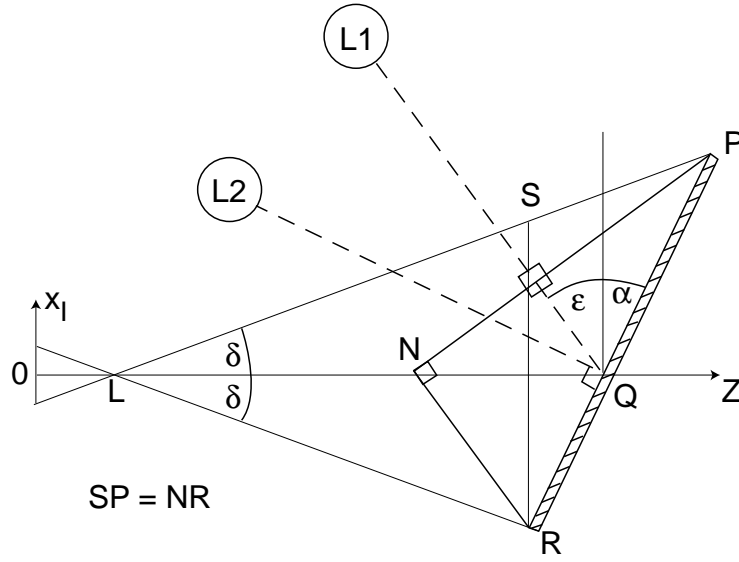
It is part of common experience that distant objects appear smaller than similar ones that are close to the observer. This is because the human visual system functions as a camera. In Fig 1 is shown a schematic camera where a number of planar objects O_A, O_B, O_C, O_D of different shape, orientation and distance produce an identical image (a square) in the image plane of the camera. The lens of the latter will be considered in the following discussion to be a simple pin-hole. If the size and orientation of the object is known then its distance l from the position L of the camera lens along the z -axis may be deduced from measurements of its image by simple geometry. For example a rod of known length r , whose centre lies on the z -axis, and is orientated parallel to Ox_I is at the distance $l = rf/r_I$ where r_I is the length of the image of the rod and f is the distance between the lens and the image plane of the camera.



CL98008Field

Figure 1: The schematic camera and the four planar objects O_A, O_B, O_C, O_D .

The problem addressed now is how the real dimensions and positions of a physical object may, in general, be deduced only from measurements made in the image plane of the camera shown in Fig 1. One possibility is to send a pulse of light with a sharp time distribution at a known time from a source near the camera and to measure the time delay and the positions of the photons scattered back into the camera. This is the principle of Radar ranging measurements. Here a different, although related, method will be used where the camera requires no external time reference. In the present Section the method will be applied to objects at rest relative to the camera, while in the following Section it



CL98009

Figure 2: The projection into the x_I - z plane of the object O_D , showing the positions in this plane of the lamps L1 and L2.

is applied to objects in uniform transverse motion with respect to the camera axis. In this case effects of Special Relativity must be taken into account.

Two different lamps L1, L2 are used to illuminate the object of interest with a sharp pulse of light whose width must be smaller than d/c where d is the typical transverse dimension of the object. The lamps L1, L2 are used as a source of correlated space-time events in the rest frame of the object of interest, that is to produce a TLO of well defined properties. They are not however essential for the following considerations. The surfaces of the objects could just as well be equipped with an array of discrete light sources (e.g. light-emitting diodes) programmed so as to emit light pulses at different values of t' , the proper time of the object, depending on their position.

The lamp L1 is situated in such a position that the photons scattered from different parts of the surface arrive simultaneously at the image plane of the camera ¹. That is the position of the lamp is such that the ‘trivial’ light propagation time differences from different parts of the object to the camera are compensated. If L1 lies in the plane spanned by the z -axis and a normal to the surface of the object, then the angle ε (Fig 2) is given by:

$$\varepsilon = \cos^{-1}\left(\frac{\sin \alpha}{\cos \delta}\right) - \alpha \quad (2.1)$$

The lamp L2 is placed along the normal to the surface of the object on the same side as the camera. Thus the scattering time of the signal from L2 corresponds to a fixed proper time in the rest frame of the (planar) object. In order that the light from the lamps may

¹This is true in the limit that δ^2 is negligible as compared to unity

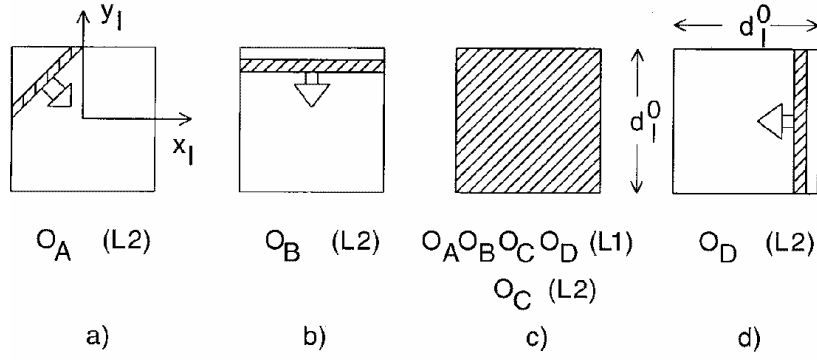


Figure 3: Images of the objects observed in the camera (viewed from the side of the objects) when lamps L1 and L2 are flashed. The arrows show the direction of motion of the instantaneous line image. The squares show the total areas swept out in the image plane by the line image. a), b), c), d) correspond to O_A , O_B , O_C and O_D for L2 whereas L1 gives the image shown in c) for all four objects.

enter the camera in the absence of specular reflection the surfaces of the objects should be diffuse reflectors. If the lamps are sufficiently distant the impinging light pulse can be considered to be a narrow planar wave packet.

For each of the objects O_A - O_D the light pulse from L1 gives a sharp (in time) square image in the camera (Fig 3c). No information is therefore available as to which of the four objects in Fig 1 produced the image. For the lamp L2, because of light propagation time differences, each object produces a clearly distinguishable image, a line moving in a distinct direction, the extremities of which sweep out the same square outline (Figs 3a,b,d) or, for O_C , an instantaneous square image indistinguishable² from that produced by the lamp L1 (Fig 3c). The orientation of the moving line image defines that of the surface of the object. It is perpendicular to the projection of the normal to the surface on to the image plane. It is now demonstrated that analysis of the time dependant images of O_A , O_B , O_D enables each object to be spatially reconstructed. Allowing for light propagation delays, the ensemble of space-time points constituting the TLO may then also be calculated.

As an example the image produced by O_D using the lamp L2 is now analysed. The times for the line to move from the right extremity of the square to the centre, and from the centre to the left extremity are denoted by Δt_1 , Δt_2 respectively. With $LQ = l$, and other geometrical definitions as in Fig 4a, then:

$$\Delta t_1^{L2} = \frac{(2ld_1 \tan \alpha - d_1^2 \sec^2 \alpha)}{c[l(1 + \cos \delta) - d_1 \tan \alpha]} \cos \delta \quad (2.2)$$

$$\Delta t_2^{L2} = \frac{(2ld_2 \tan \alpha + d_2^2 \sec^2 \alpha)}{c[l(1 + \cos \delta) + d_2 \tan \alpha]} \cos \delta \quad (2.3)$$

$$\frac{d_1}{l - d_1 \tan \alpha} = \frac{d_2}{l + d_2 \tan \alpha} = \tan \delta \quad (2.4)$$

In Eqns(2.2),(2.3) light propagation time differences inside the camera are neglected. With the further assumptions $\delta \ll 1$, $l \gg \frac{d_2}{2} \tan \alpha$, $d_2 \csc 2\alpha$ Eqns(2.2),(2.3) simplify to :

$$\Delta t_1^{L2} \simeq \frac{d_1}{c} \tan \alpha \quad (2.5)$$

$$\Delta t_2^{L2} \simeq \frac{d_2}{c} \tan \alpha \quad (2.6)$$

Denoting by d_I^0 the size of the side of the square swept out by the moving line image in Fig 3d then:

$$\frac{d_I^0}{2f} = \tan \delta \quad (2.7)$$

Eqns(2.4-2.7) have the following solution:

$$d_1 = \frac{d_I^0}{2f} c \Delta t_1 A_t^{L2} \quad (2.8)$$

²On the assumption that the transverse dimensions of the object are much larger than those of the camera and that L2 is more distant from the object than the camera, the latter will, for O_C , shadow the central region of the square image. This inessential complication does not arise if O_C is self luminous.

$$d_2 = \frac{d_I^0}{2f} c \Delta t_2 A_t^{L2} \quad (2.9)$$

$$\cot \alpha = \frac{d_I^0}{2f} A_t^{L2} \quad (2.10)$$

$$l = \frac{2c \Delta t_1^{L2} \Delta t_2^{L2}}{\Delta t_2^{L2} - \Delta t_1^{L2}} \quad (2.11)$$

where:

$$A_t^{L2} = \frac{\Delta t_1^{L2} + \Delta t_2^{L2}}{\Delta t_2^{L2} - \Delta t_1^{L2}}$$

Thus the position, orientation and physical dimensions of O_D are completely specified by measurements of Δt_1^{L2} , Δt_2^{L2} and d_I^0 , and the orientation of the moving line image. Similar calculations may be performed, *mutandis mutandi* for O_A and O_B . The object O_C is a special case. Since $\Delta t_1^{L2} = \Delta t_2^{L2} = 0$ it must be orientated perpendicular to Oz. However no information can be obtained, using the lamp L2, about its position and size.

3 Space Time Measurements of Transient Luminous Objects in Uniform Transverse Motion

The observation of the object O_D described in the previous Section is now repeated in the case that O_D and the lamps L1,L2 are moving with a constant velocity $v = \beta c$ relative to the camera and parallel to Ox_I . A coordinate system is defined in the moving frame S' with origin at Q and axes Qx' , Qy' , Qz' parallel to Ox_I , Oy_I , Oz (Fig 4). The frame, at rest relative to the camera, whose origin coincides with Q at $t = t' = 0$, and with x and y axes parallel to Ox_I and Oy_I respectively is denoted by S. It is further assumed that the light pulses from L1 and L2 arrive at Q at time $t' = 0$. To calculate the moving image observed in the camera under these conditions the light propagation times found in the previous Section may be used after first performing the LT of space-time points between the frames S and S':

$$x = \gamma(x' + vt') \quad (3.1)$$

$$t = \gamma(t' + \beta \frac{x'}{c}) \quad (3.2)$$

where

$$\gamma \equiv \frac{1}{\sqrt{1 - \beta^2}}$$

The results of the LT for the points P,Q,R of O_D are summarised in Tables 1 and 2, for observations using lamps L1 and L2 respectively, under the conditions described above. The fourth column of Table 2 is an example of the following general result (Space Dilatation) referred to in the introduction:

A transient luminous object, lying along the Ox' axis, whose length in S' at fixed time t' is d , appears if observed in S with coarse time resolution to be of length γd .

As discussed in detail below, the time resolved image is, just as in the case of a

Point on object	x'	t'	x	t
P	d_2	$-\frac{d_2}{c} \tan \alpha$	$\gamma d_2(1 - \beta \tan \alpha)$	$\gamma \frac{d_2}{c}(\beta - \tan \alpha)$
Q	0	0	0	0
R	$-d_1$	$\frac{d_1}{c} \tan \alpha$	$-\gamma d_1(1 - \beta \tan \alpha)$	$-\gamma \frac{d_1}{c}(\beta - \tan \alpha)$

Table 1: Space-time points on the object O_D , illuminated by a short light pulse from the lamp L1 (Fig.2), as observed in the frames S',S.

Point on object	x'	t'	x	t
P	d_2	0	γd_2	$\frac{\gamma v d_2}{c^2}$
Q	0	0	0	0
R	$-d_1$	0	$-\gamma d_1$	$-\frac{\gamma v d_1}{c^2}$

Table 2: Space-time points on the object O_D , illuminated by a short light pulse from the lamp L2 (Fig.2), as observed in the frames S',S.

stationary object, a vertical line moving parallel to Ox_I . The meaning of ‘coarse’ time resolution will also be quantified.

Including both the effects of the LT and of the light propagation delays, Δt_1 , Δt_2 are given, in the case that O_D is moving transversely, by the equations :

$$\Delta t_1^{L1} = -\frac{\gamma d_1}{c}(\tan \alpha - \beta) + \frac{d_1}{c} \frac{\{2 \tan \alpha - r_1[\gamma^2(1 - \beta \tan \alpha)^2 + \tan^2 \alpha]\}}{1 + \sqrt{\gamma^2(1 - \beta \tan \alpha)^2 r_1^2 + (1 - r_1 \tan \alpha)^2}} \quad (3.3)$$

$$\Delta t_2^{L1} = -\frac{\gamma d_2}{c}(\tan \alpha - \beta) + \frac{d_2}{c} \frac{\{2 \tan \alpha + r_2[\gamma^2(1 - \beta \tan \alpha)^2 + \tan^2 \alpha]\}}{1 + \sqrt{\gamma^2(1 - \beta \tan \alpha)^2 r_2^2 + (1 + r_2 \tan \alpha)^2}} \quad (3.4)$$

$$\Delta t_1^{L2} = \frac{d_1 \gamma \beta}{c} + \frac{d_1[2 \tan \alpha - r_1(\gamma^2 + \tan^2 \alpha)]}{1 + \sqrt{\gamma^2 r_1^2 + (1 - r_1 \tan \alpha)^2}} \quad (3.5)$$

$$\Delta t_2^{L2} = \frac{d_2 \gamma \beta}{c} + \frac{d_2[2 \tan \alpha + r_2(\gamma^2 + \tan^2 \alpha)]}{1 + \sqrt{\gamma^2 r_2^2 + (1 + r_2 \tan \alpha)^2}} \quad (3.6)$$

where

$$r_1 = d_1/l, \quad r_2 = d_2/l$$

On setting $\beta = 0, \gamma = 1$ in Eqns(3.5),(3.6) Eqns(2.2),(2.3) are recovered. In Eqns(3.3)-(3.6) the first terms on the right hand sides are the time shifts due to the LT, while the second terms account for light propagation delays between the object and the camera. The γ, β dependent terms in the latter are also a consequence of the LT, that changes the

apparent size of the object (see the fourth column of Tables 1 and 2) and so effects also the light propagation delays.

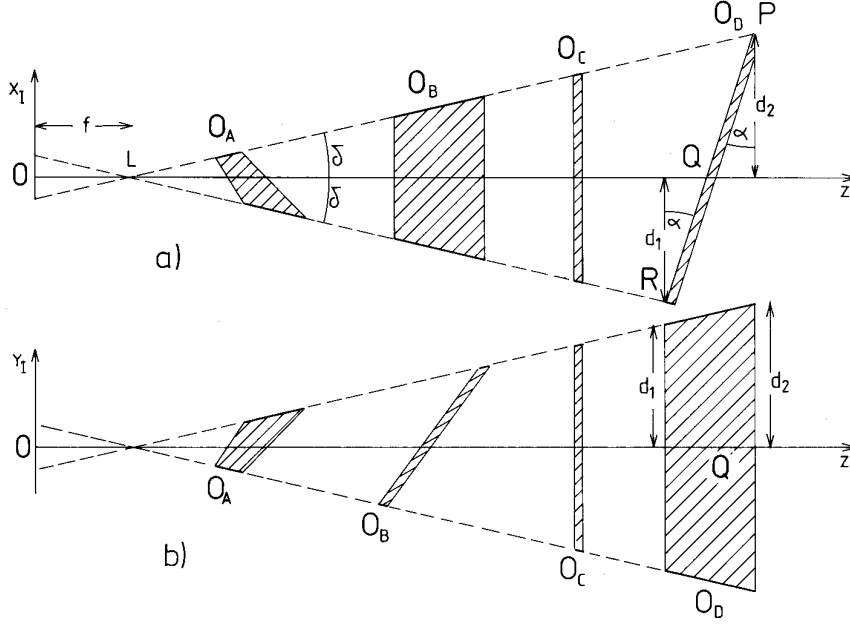


Figure 4: a) x_I - z projections, b) y_I - z projections of the four planar objects and the camera.

The images observed in the camera are now discussed in two extreme limits. In the first a similar approximation is made to that used in deriving Eqns(2.5),(2.6) from (2.2),(2.3). All terms containing r_1, r_2 in Eqns (3.3)-(3.6) are neglected. This is a good approximation for not too large γ (say $\beta \leq 0.9, \gamma \leq 2$) and $\tan \alpha, d_1, d_2 \ll l$. The second is the ultrarelativistic limit $\gamma \gg 1$. In the small $\gamma, \tan \alpha$ limit Eqns (3.3)-(3.6) simplify to :

$$\Delta t_i^{L1} = -\frac{d_i}{c}[(\gamma - 1) \tan \alpha - \gamma \beta] \quad i = 1, 2 \quad (3.7)$$

$$\Delta t_i^{L2} = \frac{d_i}{c}[\tan \alpha + \gamma \beta] \quad i = 1, 2 \quad (3.8)$$

It is convenient to introduce the quantities d_I for the width of the image observed with coarse time resolution and $\Delta t = \Delta t_1 + \Delta t_2$ the full time over which the moving image exists. The quantity $\beta_I = d_I/c\Delta t$ is the average velocity, in units of c , of the moving line image. From Tables 1 and 2 and Eqns(3.7), (3.8) these quantities are:

$$d_I^{L1} = \gamma(1 - \beta \tan \alpha)d_I^0 \quad (3.9)$$

$$d_I^{L2} = \gamma d_I^0 \quad (3.10)$$

$$\Delta t^{L1} = -\frac{(d_1 + d_2)}{c}[(\gamma - 1) \tan \alpha - \beta \gamma] \quad (3.11)$$

$$\Delta t^{L2} = \frac{(d_1 + d_2)}{c}[\tan \alpha + \beta \gamma] \quad (3.12)$$

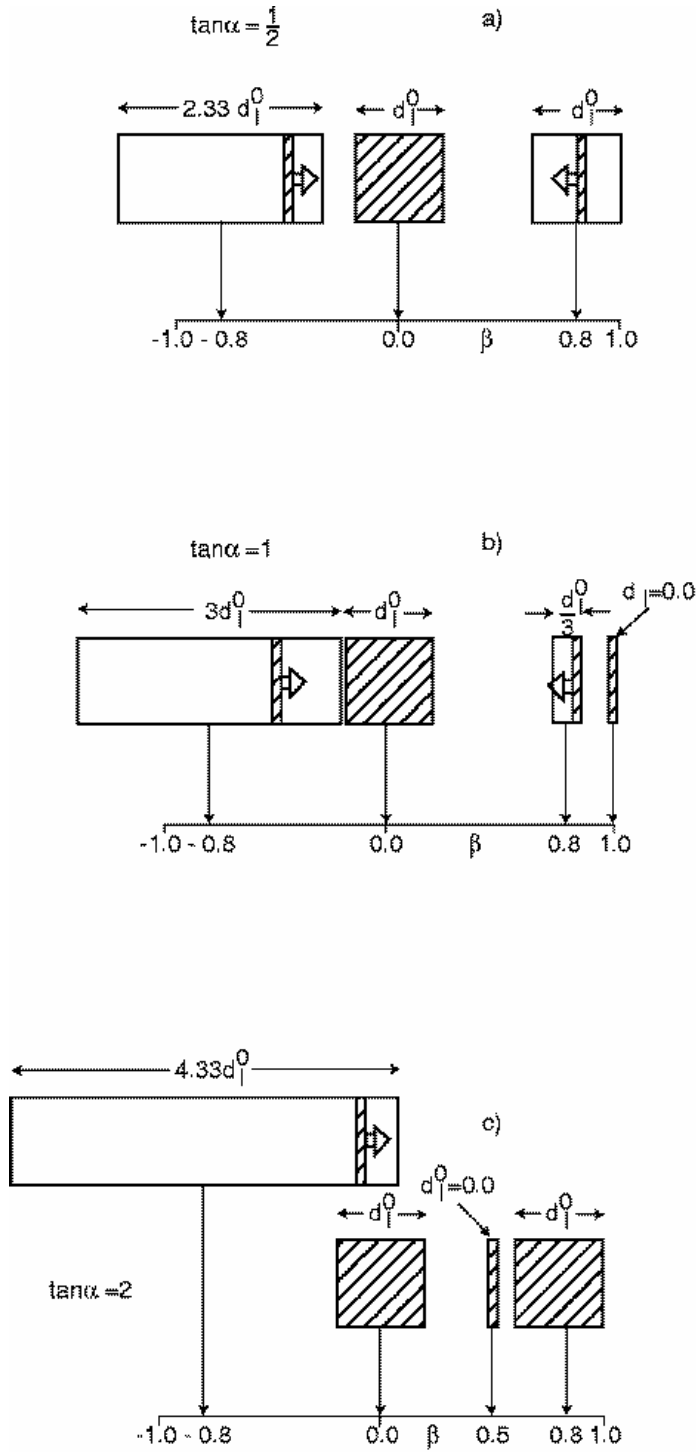


Figure 5: Images of O_D observed when the lamp L1 is flashed while L1 and O_D are in uniform motion relative to the camera with velocity βc parallel to O_{x_I} . a), b), c) correspond to $\tan \alpha = 1/2, 1, 2$ respectively. Comments as for Fig.3.

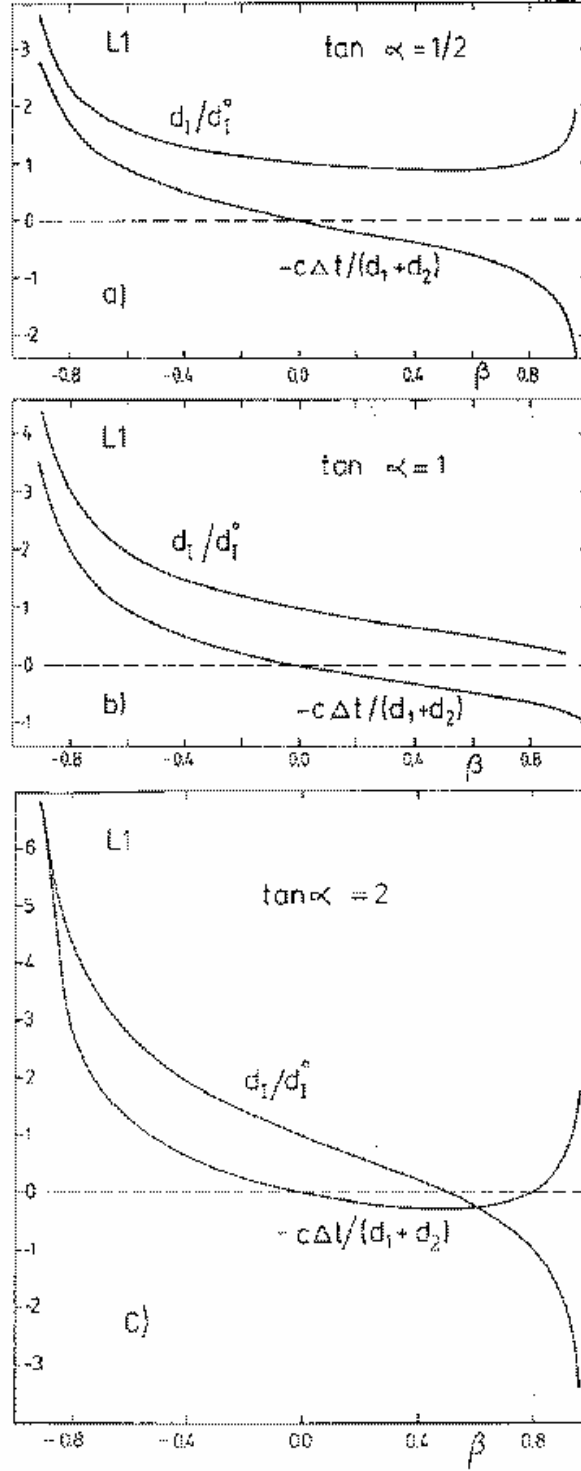


Figure 6: d_I/d_I^0 and $-c\Delta t/(d_1+d_2)$ as a function of β for the conditions of Fig.5. d_I is the width parallel to O_{x_I} of the rectangle in Fig.5, i.e. the width of the image when observed with coarse time resolution. Δt is the total duration of the moving image. a),b),c) are for $\tan \alpha = 1/2, 1, 2$ respectively.

where

$$d_I^0 = f \frac{(d_1 + d_2)}{l} \quad (3.13)$$

The quantity d_I^0 , introduced in the previous section, is the side of the square swept out by each moving image when $\beta = 0$ (see Fig 3). Typical images for L1 for different values of β and for $\tan \alpha = 1/2, 1, 2$ are shown in Figs 5a,b,c respectively. The corresponding plots of the quantities d_I/d_I^0 and $-c\Delta t/(d_1 + d_2)$ as a function of β are shown in Figs 6a,b,c. The convention in Fig 5 is the same as in Fig 3, the images are viewed from the object side and the dashed rectangles or squares indicate the full areas swept out by the moving line images. It is evident from Figs 5 and 6 that the images have a complicated structure as a function of β , but qualitatively they do not differ from those of a similar object at rest. For $\beta > 0$ (< 0) the line image moves to the left (right). For $\tan \alpha < 1$ d_I^{L1} has a minimum value when $\beta = \tan \alpha$:

$$d_I^{L1,MIN} = d_I^0 \sqrt{1 - \tan^2 \alpha} \quad (3.14)$$

while for $\tan \alpha > 1$, Δt has a maximum when $\beta = 1/\tan \alpha$:

$$\Delta t^{L1,MAX} = \frac{(d_1 + d_2)}{c} \left[\frac{\sqrt{\tan^2 \alpha - 1}}{\tan \alpha} - \tan \alpha \right] \quad (3.15)$$

For $\tan \alpha > 1$, d_I vanishes for some positive value of β (Figs. 5c,6c), and Δt has a second zero for positive β (by construction, it of course vanishes for $\beta = 0$ and any α). When $\tan \alpha = 2$, Δt vanishes for $\beta = 0.8$. The instantaneous image is then identical to that obtained for $\beta = 0$. It is easily shown, using Eqns.(3.9),(3.11), that the same instantaneous image is obtained when $\Delta t = 0$ for any $\tan \alpha > 1$. Note that, because of the approximations made above, Eqns.(3.9),(3.11) are not valid for $\beta \simeq 1$ (see the discussion of the ultra-relativistic limit where $|\beta| \simeq 1$ below).

The structure of the images is simpler for the case of the lamp L2 (Figs.7 and 8). d_I^{L2} has the constant value γd_I^0 independant of α . Since this is an example of Space Dilation the only relevant parameter is the total extension of the object along the Ox' axis. For $\gamma\beta > -\tan \alpha$ ($\gamma\beta < -\tan \alpha$) the line image moves to the left (right), see Fig 7. At $\gamma\beta = -\tan \alpha$ (Figs. 7,8) then $\Delta t = 0$ and an instantaneous rectangular image is seen. The minimum value of d_I of d_I^0 occurs when $\beta = 0$. Δt is an increasing monotonic function of β for all values of β .

The form of the images in the Ultra-Relativistic (UR) limit $|\beta| \simeq 1$ will now be discussed. In this case only the γ dependent terms in Eqns.(3.3)-(3.6) are retained, leading to the expressions:

$$\Delta t^{L1} = \frac{\gamma}{c} [(d_1 + d_2)(\beta - \tan \alpha) + (d_1 + d_2)(\beta \tan \alpha - 1)] \quad (3.16)$$

$$\Delta t^{L2} = \gamma [d_2(1 + \beta) - d_1(1 - \beta)] \quad (3.17)$$

while Eqns.(3.9),(3.10), being exact, remain valid. For lamp L1 different behaviour in the UR limit occurs for $\tan \alpha \neq \pm 1$ and $\tan \alpha = \pm 1$. For $\tan \alpha \neq \pm 1$, Eqns.(3.9),(3.16) give $|d_I^{L1}|, |\Delta t^{L1}| \rightarrow \infty$ as $|\beta| \rightarrow 1$. The velocity β_I is however finite and independent, for $|\beta| = 1$, of $\tan \alpha$. In general, in the UR limit :

$$\beta_I^{L1} = \frac{d_I}{c\Delta t} = \frac{(1 - \beta \tan \alpha)d_I^0}{[(d_1 + d_2)(\beta - \tan \alpha) + (d_1 - d_2)(\beta \tan \alpha - 1)]} \quad (3.18)$$

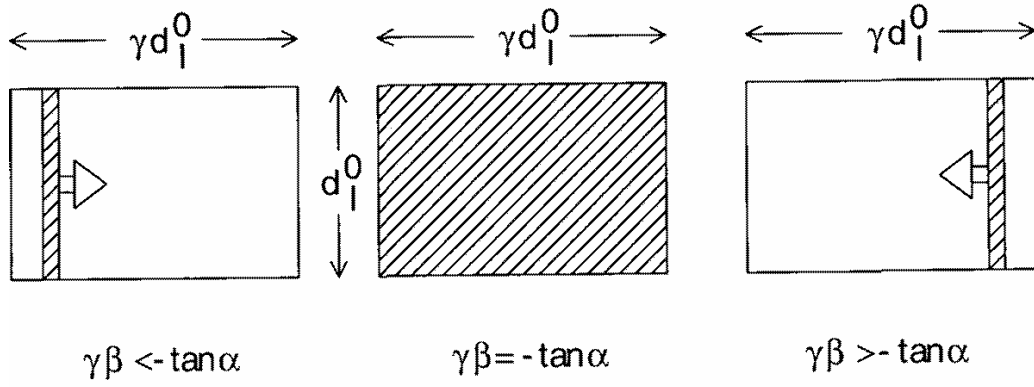
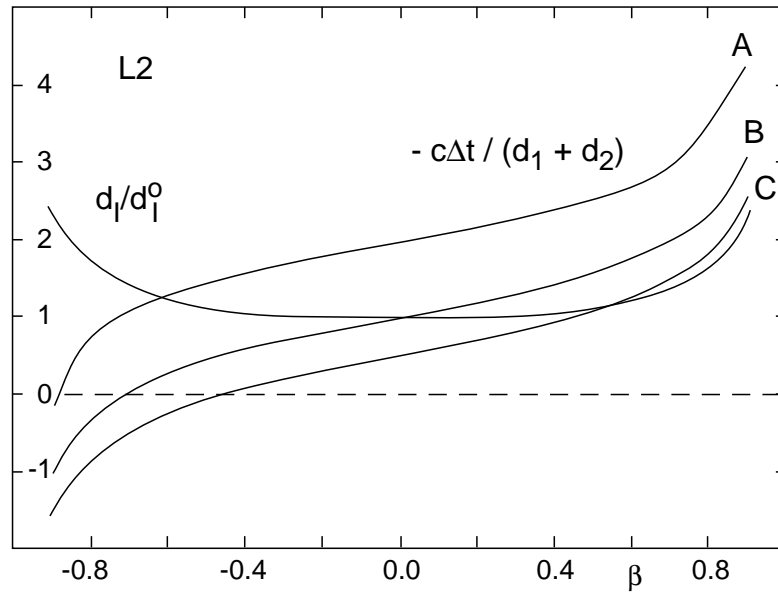


Figure 7: Images of O_D observed when lamp L2 is flashed and L2 and O_D move uniformly relative to the camera with velocity βc parallel to O_{x_I} . Comments as for Fig.3.



CL98015

Figure 8: d_I/d_I^0 and $-c\Delta t/(d_1 + d_2)$ (Curves A, B, C) as a function of β for the conditions of Fig.7 (lamp L2 flashed). Curves A,B,C for $\tan \alpha = 1/2, 1, 2$ respectively.

	$\tan \alpha \neq \pm 1$		$\tan \alpha = 1$		$\tan \alpha = -1$	
	$\beta \rightarrow 1$	$\beta \rightarrow -1$	$\beta \rightarrow 1$	$\beta \rightarrow -1$	$\beta \rightarrow 1$	$\beta \rightarrow -1$
$ d_I^{L1} $	∞	∞	0	∞	∞	0
$ \Delta t^{L1} $	∞	∞	0	∞	∞	0
β_I^{L1}	$\frac{f}{2l}(1 + \frac{d_1}{d_2})$	$-\frac{f}{2l}(1 + \frac{d_2}{d_1})$	$-\frac{f}{2l}(1 + \frac{d_2}{d_1})$	$-\frac{f}{2l}(1 + \frac{d_2}{d_1})$	$\frac{f}{2l}(1 + \frac{d_1}{d_2})$	$\frac{f}{2l}(1 + \frac{d_1}{d_2})$

Table 3: The size $|d_I^{L1}|$, time duration $|\Delta t^{L1}|$ and velocity parallel to Ox_I β_I^{L1} , of images of the object O_D , illuminated by the lamp L1 for different values of $\tan \alpha$ in the UR limit.

so

$$\beta_I^{L1}(\beta = 1) = \frac{f}{2l}(1 + \frac{d_1}{d_2}) \quad (\tan \alpha \neq \pm 1) \quad (3.19)$$

and

$$\beta_I^{L1}(\beta = -1) = -\frac{f}{2l}(1 + \frac{d_2}{d_1}) \quad (\tan \alpha \neq \pm 1) \quad (3.20)$$

For $\tan \alpha = 1$, (3.7), (3.16) give

$$d_I^{L1}(\tan \alpha = 1) = \sqrt{\frac{1-\beta}{1+\beta}} d_I^0 \quad (3.21)$$

$$\Delta t^{L1}(\tan \alpha = 1) = -\frac{2}{c} \sqrt{\frac{1-\beta}{1+\beta}} d_1 \quad (3.22)$$

so that, with Eqn.(3.13):

$$\beta_I^{L1}(\tan \alpha = 1) = -\frac{f}{2l}(1 + \frac{d_2}{d_1}) \quad (3.23)$$

whereas for $\tan \alpha = -1$, one obtains:

$$d_I^{L1}(\tan \alpha = -1) = \sqrt{\frac{1+\beta}{1-\beta}} d_I^0 \quad (3.24)$$

$$\Delta t^{L1}(\tan \alpha = -1) = \frac{2}{c} \sqrt{\frac{1+\beta}{1-\beta}} d_2 \quad (3.25)$$

and hence

$$\beta_I^{L1}(\tan \alpha = -1) = \frac{f}{2l}(1 + \frac{d_1}{d_2}) \quad (3.26)$$

Thus d_I^{L1} and Δt^{L1} , for $\tan \alpha = 1$, vanish as $\beta \rightarrow 1$ and are infinite as $\beta \rightarrow -1$. On the contrary, d_I^{L1} and Δt^{L1} , for $\tan \alpha = -1$, are infinite as $\beta \rightarrow 1$ and vanish as $\beta \rightarrow -1$. For $\tan \alpha = 1$ the limiting velocity is the same as for $\tan \alpha \neq 1$ and $\beta = -1$, while for $\tan \alpha = -1$ it is the same as for $\tan \alpha \neq 1$ and $\beta = 1$. The UR limits for lamp L1 in all the cases discussed above are summarised in Table 3.

As there is no $\tan \alpha$ dependence the UR limits for the lamp L2 are simpler. For $|\beta| \rightarrow 1$, d_I^{L2} always diverges to $+\infty$, whereas Δt^{L2} diverges to $+\infty$ as $\beta \rightarrow 1$ and to

	$\beta \rightarrow 1$	$\beta \rightarrow -1$
d_I^{L2}	∞	∞
Δt^{L2}	∞	$-\infty$
β_I^{L2}	$\frac{f}{2l}(1 + \frac{d_1}{d_2})$	$-\frac{f}{2l}(1 + \frac{d_2}{d_1})$

Table 4: The size $|d_I^{L2}|$, time duration $|\Delta t^{L2}|$ and velocity (parallel to Ox_I) β_I^{L2} , of images of the object O_D , illuminated by the lamp L2 in the UR limit.

$-\infty$ as $\beta \rightarrow -1$. The same limiting velocities are found as $\beta \rightarrow \pm 1$ as for lamp L1 when $\tan \alpha = \mp 1$. These results are summarised in Table 4. It may be remarked that for $\tan \alpha \neq \pm 1$ lamps L1 and L2 give similar, infinitely wide, images in the UR limit.

In the above discussion optical aberration has been neglected and it is assumed that the camera is still sensitive for large values of β where the observed photons have a large red-shift. Denoting by θ, θ' the angles in the S, S' frames of the diffusely reflected photons relative to the x, x' axes, the LT of the photon momentum leads to the relation :

$$\tan \theta = \frac{\sin \theta'}{\gamma(\cos \theta' + \beta)} \quad (3.27)$$

In order to enter the camera the photons must have $\theta \simeq \frac{\pi}{2}$, implying from Eqn.(3.27) that $\cos \theta' \simeq -\beta$. If $\theta' > \pi - \alpha$, then (see Fig2.) the photons cannot be diffusely reflected from the surface of the object. This leads, for any value of α , to a maximum value of β for diffuse reflection. For $\tan \alpha = 1/2, 1, 2$ as in Figs.5,6 $\beta_{MAX} = 0.88, 0.707, 0.440$. If the object is translucent, or equipped with a lamp similarly situated to L1, but illuminating the back surface of the object (i.e. placed at the position the mirror image of L1 in the object) then the above limitation is avoided. For $\beta > \beta_{MAX}$ the photons entering the camera originate entirely from reflection on the surface remote from the camera. This is just the optical aberration effect referred to in the Introduction that leads to the apparent rotation of rapidly moving objects [2, 3, 4]. No such restriction applies for negative values of β and in this case the photons are always reflected from the front surface of the object.

Since (compare Figs.3,5,7) the images of stationary and moving TLO are not distigishable, and the moving image is defined by just three independent quantities (say $\Delta t_1, \Delta t_2$ and d_I) whereas four (for example d_1, α, l and v) are needed to completely specify the moving planar object, image plane measurements using only one lamp do not enable reconstruction of the object. It suffices however to perform measurements, under identical conditions, using separately L1 and L2 to derive the true dimensions, orientation, position and velocity of the object³. From Eqns.(3.9,3.10):

$$r_d \equiv \frac{d_I^{L1}}{d_I^{L2}} = 1 - \beta \tan \alpha \quad (3.28)$$

³ In general equivalent information is provided by any two lamps situated in the plane defined by the optic axis of the camera and the normal to the surface of the object at different known angular positions with respect to the normal.

and from Eqns.(3.11),(3.12)

$$r_t \equiv \frac{\Delta t^{L1}}{\Delta t^{L2}} = \frac{\beta\gamma - (\gamma - 1) \tan \alpha}{\tan \alpha + \beta\gamma} \quad (3.29)$$

Eliminating $\tan \alpha$ between Eqns.(3.28) and (3.29) and solving for γ gives:

$$\gamma = \sqrt{r_3^2 + r_4 - r_3} \quad (3.30)$$

where

$$r_3 \equiv \frac{(1 - r_d)(1 - r_t)}{2(r_d - r_t)}, \quad r_4 \equiv \frac{(1 - r_t)}{r_d - r_t}$$

Re-writing Eqn.(3.28), $\tan \alpha$ is then given by:

$$\tan \alpha = \frac{\gamma}{\sqrt{\gamma^2 - 1}}(1 - r_d) \quad (3.31)$$

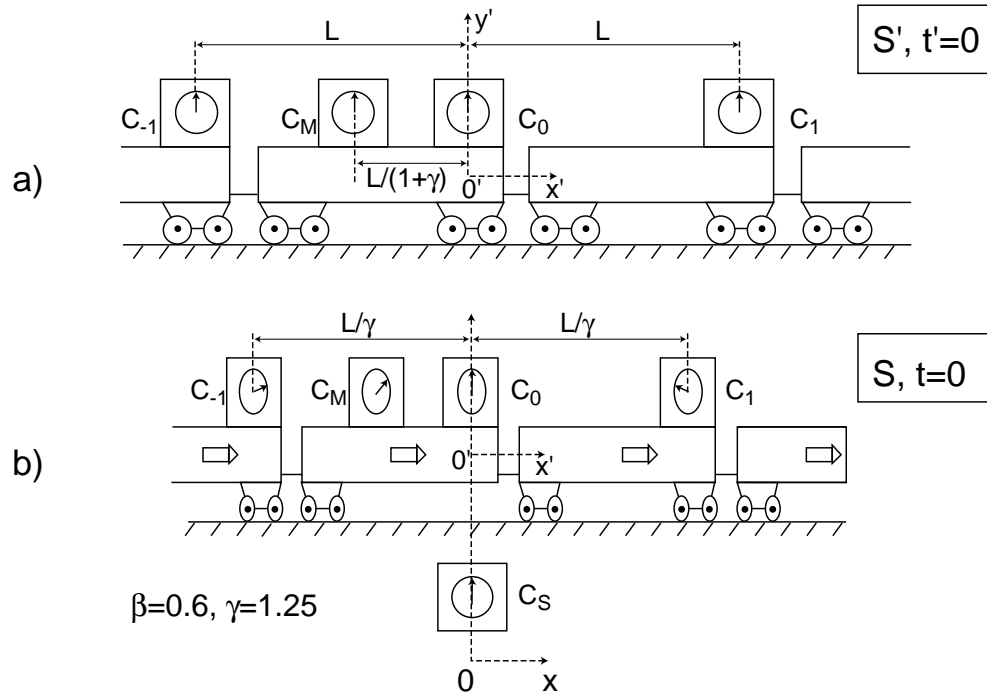
Since $\tan \alpha$, β , γ are now known, d_1 and d_2 may be determined from Eqns.(3.7) or (3.8). Finally, l is given by the relation:

$$l = \frac{2d_1d_2 \tan \alpha}{d_2 - d_1} \quad (3.32)$$

Thus by combining measurements made under similar conditions, using lamps L1 and L2 a complete specification of the moving object is obtained using only the IPC information.

4 Space Time Measurements of Equivalent Moving Clocks

In this Section space time measurements of an array of synchronised clocks situated in the inertial frame S' will be considered. These clocks may be synchronised by any convenient procedure ⁴ (see for example Ref.[1]). For an observer in S' all such clocks are 'equivalent' in the sense that each of them records, independently of its position, the proper time τ' of the frame S'. For convenience, the array of clocks is assumed to be placed on the wagons of a train which is at rest in S', as shown in Fig.9a. The clocks are labelled C_m , $m = \dots - 2, -1, 0, 1, 2, \dots$ and are situated (with the exception of the 'magic clocks' C_M, \overline{C}_M , see below) at fixed distances L from each other, along the Ox' axis, which is parallel to the train. Any observer in S' will, after making the necessary corrections for Light Propagation Time Delays (LPTD), note that each Equivalent Clock (EC) indicates the same time, as shown in Fig.9a. It is now asked how the array of EC will appear to an observer at a fixed position in the frame S when the train is moving with velocity βc parallel to the direction Ox in S (Fig.9b). It is assumed that the EC C_0 is placed at $x' = 0$ and that it is synchronised with the Standard Clock C_S , placed at



CL98016

Figure 9: a) Positions and times of equivalent clocks on the wagons of a train as seen by observers in the rest frame S' of the train (without the effects of LPTD). b) The positions and times of the same clocks as seen by an observer in S (without the effects of LPTD). In S the train is moving to the right with velocity βc .

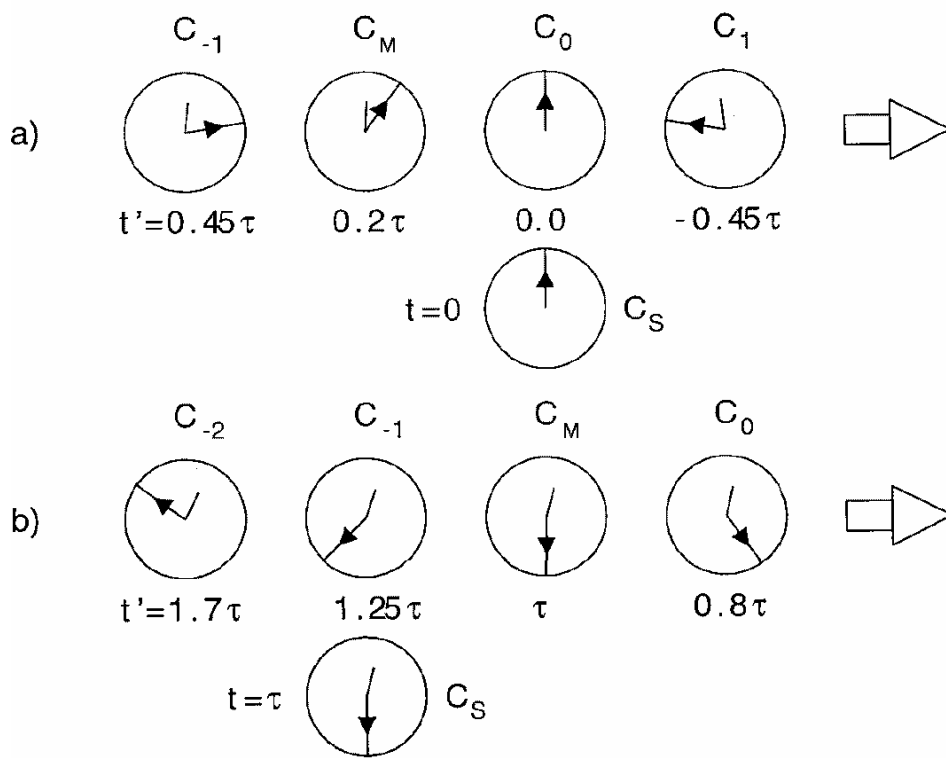


Figure 10: Equivalent clocks on the train as seen by an observer in S. a) at $t = 0$, b) at $t = \tau$ (without the effects of LPTD).

C_S	C_{-2}	C_{-1}	C_M	C_0	C_1	C_2
0	$2\frac{(\gamma^2-1)}{\gamma}\tau$	$\frac{(\gamma^2-1)}{\gamma}\tau$	$\frac{(\gamma-1)}{\gamma}\tau$	0	$-\frac{(\gamma^2-1)}{\gamma}\tau$	$-2\frac{(\gamma^2-1)}{\gamma}\tau$
τ	$\frac{(2\gamma^2-1)}{\gamma}\tau$	$\gamma\tau$	τ	$\frac{\tau}{\gamma}$	$-\frac{(\gamma^2-2)}{\gamma}\tau$	$-\frac{(2\gamma^2-3)}{\gamma}\tau$

Table 5: Apparent times of Equivalent Clocks on the moving train in Fig.9, at times $t = 0$ and $t = \tau$ of the stationary standard clock C_S . Effects of the LT only.

$x = 0$ in S, when $t = t' = 0$. The EC C_m and C_S record exactly equal time intervals when they are situated in the same inertial frame.

The appearance of the moving EC to an observer in S (after correction for LPTD; their actual appearance, including this effect, is considered later) at $t = 0$ is shown in Fig.9b, and in more detail in Fig.10 for both $t = 0$ and $t = \tau$. The period τ is the time between the passage of successive EC past C_S . The big hand of C_S in Fig.10 rotates through 180° during the time τ . Explicit expressions for the apparent times are presented in Table 5. In Fig.9b,10 the times indicated by the clocks are shown for $\beta = 0.6$. These apparent times are readily calculated using the LT equations (3.1),(3.2). Consider the time indicated by C_1 at $t = 0$. The space-time points are:

$$S' : (L, t') ; \quad S : (x, 0)$$

Hence, Eqns.(3.1),(3.2) give:

$$x = \gamma(L + vt') \tag{4.1}$$

$$0 = \gamma(t' + \frac{\beta L}{c}) \tag{4.2}$$

which have the solution [$C_1(t = 0)$]:

$$t' = -\frac{\beta L}{c} \tag{4.3}$$

$$x = \frac{L}{\gamma} \tag{4.4}$$

As shown in Fig 9b, the wagons of the train are apparently shorter due to the LFC effect (Eqn.(4.4)) and also *the wagons at the front end of the train are seen at an earlier time than those at the rear end*. Thus a $t = 0$ snapshot in S corresponds, not to a fixed t' in S' but one which depends on x' : $t' = -\beta x'/c$. This is a consequence of the relativity of simultaneity of space-time events in S and S', as first pointed out by Einstein in Ref.[1]. Here it appears in a particularly graphic and striking form. The part of the space-time domain in S' that may be observed from S is considered in detail below. Consider now the time indicated by C_{-1} at $t = \tau$, i.e. when C_{-1} is at the origin of S. The space-time points are:

$$S' : (-L, t') ; \quad S : (0, \tau)$$

⁴If an observer in S' knows the distance D to any of the clocks then the clock is synchronised relative to a local clock at the same position as the observer, when it is observed to lag behind the latter by the time D/c when viewed across free space

C_S	C_{-2}	C_{-1}	C_M	C_0	C_1	C_2
0	$-2\gamma\beta\tau$	$-\gamma\beta\tau$	$\left[\sqrt{(1-\beta)/(1+\beta)} - 1\right]\tau$	0	$-\gamma\beta\tau$	$-2\gamma\beta\tau$
τ	$\gamma(1-\beta)\tau$	$\gamma\tau$	τ	$\gamma(1-\beta)\tau$	$\gamma(1-2\beta)\tau$	$\gamma(1-3\beta)\tau$

Table 6: Definitions as for Table 5, except that the effects of LPTD for an observer close to the train are also included.

Hence, Eqns.(3.1),(3.2) give:

$$0 = \gamma(-L + vt') \quad (4.5)$$

$$\tau = \gamma\left(t' - \frac{\beta L}{c}\right) \quad (4.6)$$

with the solutions [$C_{-1}(t = \tau)$]:

$$t' = \frac{L}{v} \quad (4.7)$$

$$\tau = \frac{L}{\gamma v} = \frac{t'}{\gamma} \quad (4.8)$$

so that

$$t' = \gamma\tau \quad (4.9)$$

The EC at the origin of S at $t = \tau$ indicates a later time than C_S i.e. it is apparently running *faster* than C_S . This is an example of Time Contraction (TC). As shown below *TC is exhibited by the EC at any fixed position in S*. In fact, if the observer in S can see the EC only when they are near to C_S he (or she) will inevitably conclude that the clocks on the train run fast, not slow as in the classical TD effect (see below). Suppose that the observer is sitting in a waiting room with the clock C_S and notices the time on the train (the same as C_S) by looking at C_0 as it passes the waiting room window. If he (or she) then compares C_{-1} as it passes the window with C_S it will be seen to be running fast relative to the latter. In order to see the TD effect the observer would (as will now be shown), have to note the time shown by, for example C_0 , at time $t = \tau$ as recorded by C_S . Indeed, to do this he would first have to correct his observation for the LPTD between himself and C_0 . At time $t = \tau$ at C_S he would actually see C_0 as it appeared at an earlier time to a nearby observer in S. Using Eqn.(4.8),Eqn.(4.3) may be written as [$C_1(t = 0)$]:

$$t' = -\beta^2\gamma\tau = -\frac{(\gamma^2 - 1)\tau}{\gamma} \quad (4.10)$$

This is the formula for the apparent time reported in Table 5. Now consider C_0 at time $t = \tau$. The space-time points are:

$$S' : (0, t') ; \quad S : (x, \tau)$$

Hence, Eqns.(3.1),(3.2) give:

$$x = \gamma vt' \quad (4.11)$$

$$\tau = \gamma t' \quad (4.12)$$

C_S	C_{-2}	C_{-1}	C_M	C_0	C_1	C_2
0	$2\frac{(\gamma^2-1)}{\gamma}\tau$	$\frac{(\gamma^2-1)}{\gamma}\tau$	$\frac{(\gamma-1)}{\gamma}\tau$	0	$-\frac{(\gamma^2-1)}{\gamma}\tau$	$-2\frac{(\gamma^2-1)}{\gamma}\tau$
τ	$\frac{(2\gamma^2-1)}{\gamma}\tau$	$\gamma\tau$	τ	$\frac{\tau}{\gamma}$	$-\frac{(\gamma^2-2)}{\gamma}\tau$	$-\frac{(2\gamma^2-3)}{\gamma}\tau$

Table 7: Apparent times of Equivalent Clocks on the moving train in Fig.9, at times $t = 0$ and $t = \tau$ of the stationary standard clock C_S . Effects of the LT only.

with the solutions [$C_0(t = \tau)$]:

$$t' = \tau/\gamma \quad (4.13)$$

$$x = v\tau = L/\gamma \quad (4.14)$$

So the EC C_0 at time $t = \tau$ indicates an earlier time, and so is apparently running slower than C_S . This is the classical Time Dilatation (TD) effect. It applies to observations of all *local clocks in S'* , (i.e. those situated at a fixed value of x') as well as any other EC that has the same value of x' .

As a last example consider the ‘Magic Clock’ C_M shown in Fig 9a at time $t = \tau$. With the space-time points:

$$S' : (-L/(1+\gamma), t') ; \quad S : (x, \tau)$$

Eqns.(3.1),(3.2) give:

$$x = \gamma[-L/(1+\gamma) + vt'] \quad (4.15)$$

$$\tau = \gamma[t' - \frac{\beta}{c}L/(1+\gamma)] \quad (4.16)$$

with the solutions [$C_M(t = \tau)$]:

$$t' = \tau \quad (4.17)$$

$$x = \gamma v\tau/(1+\gamma) \quad (4.18)$$

where the relation $L = \gamma v\tau$ from Eqn.(4.14) has been used. Thus C_M indicates the same time as C_S at $t = \tau$. Similar ‘Magic Clocks’ can be defined that show the same time as C_S at any chosen time t in S . Such a clock is, in general, situated at $x' = -ct(\gamma - 1)/\beta\gamma$. All of the other apparent times presented in Table 5 and shown in Figs. 9b, 10 are calculated in a similar way to the above examples by choosing appropriate values of x' and t .

It is straightforward to derive a general formula for the apparent time of any EC, C_m after the passage of an arbitrary number j of wagons past the clock C_S . Still neglecting LPTD, the result is :

$$t'_{m,j} = -\frac{[m\gamma^2 - (m+j)]\tau}{\gamma} \quad (4.19)$$

A consequence of (4.19) is :

$$t'_{m,j+1} - t'_{m,j} = \tau/\gamma \quad (4.20)$$

This is the general TD result for any local ($x' = \text{constant}$) EC C_m . Eqn.(4.19) may, alternatively, be written in terms of (n, j) where the index n labels the position of an EC in S rather than in S'. So the clocks at $x = L/\gamma, 2L/\gamma, \dots$ (see Fig. 9b) have $n = 1, 2, \dots$, those with $x = -L/\gamma, -2L/\gamma, \dots$ have $n = -1, -2, \dots$. Using the general relation :

$$n = m + j \quad (4.21)$$

Eqn.(4.19) may be written as :

$$t'_{n,j} = -\frac{[(n-j)\gamma^2 - n]\tau}{\gamma} \quad (4.22)$$

so that

$$t'_{n,j+1} - t'_{n,j} = \gamma\tau \quad (4.23)$$

This is the general TC effect for an EC at fixed n ($x = \text{constant}$). Eqn.(4.22) may also be used to calculate the apparent time delay between the EC on successive wagons at a fixed time in S :

$$t'_{n+1,j} - t'_{n,j} = -\gamma\beta^2\tau \quad (4.24)$$

The effects of LPTD on the apparent times indicated by the clocks on the moving train will now be taken into account. Only propagation times parallel to the train are considered and it is assumed that the clocks are orientated in such away that they can be seen by an observer placed beside C_S . Consider the clock C_n at the time Δt before the passage of the j th wagon past C_S (Fig.11). If the clock m is at the position x_m in S at this time then the inverse of the LT Eqn.(3.1) gives:

$$mL = \gamma[x_m - v(j\tau - \Delta t)] \quad (4.25)$$

The corresponding time shown by C_m , $t'^D_{m,j}$ is, using the inverse of the LT Eqn.(3.2):

$$t'^D_{m,j} = \gamma[j\tau - \Delta t - \frac{\beta x_m}{c}] \quad (4.26)$$

There are now two cases to consider:

- (i) $x_m > 0$, C_m receding from the observer;
- (i) $x_m < 0$, C_m approaching the observer;

If $|x_m| = c\Delta t$ the observer beside C_S in S will see the time $t'^D_{m,j}$ indicated by the clock C_m at time $j\tau$. Since Δt is, by definition, positive then in case (i) above x_m in (4.25) and (4.26) is replaced by $c\Delta t$. Eliminating Δt between the equations, after this replacement, gives for the apparent time:

$$t'^D_{m,j} = \gamma[j(1 - \beta) - \beta m]\tau \quad (x_m > 0) \quad (4.27)$$

In case (ii) x_m in Eqns.(4.25),(4.26) is replaced by $-c\Delta t$, giving the solution:

$$t'^D_{m,j} = \gamma[j(1 + \beta) + \beta m]\tau \quad (x_m < 0) \quad (4.28)$$

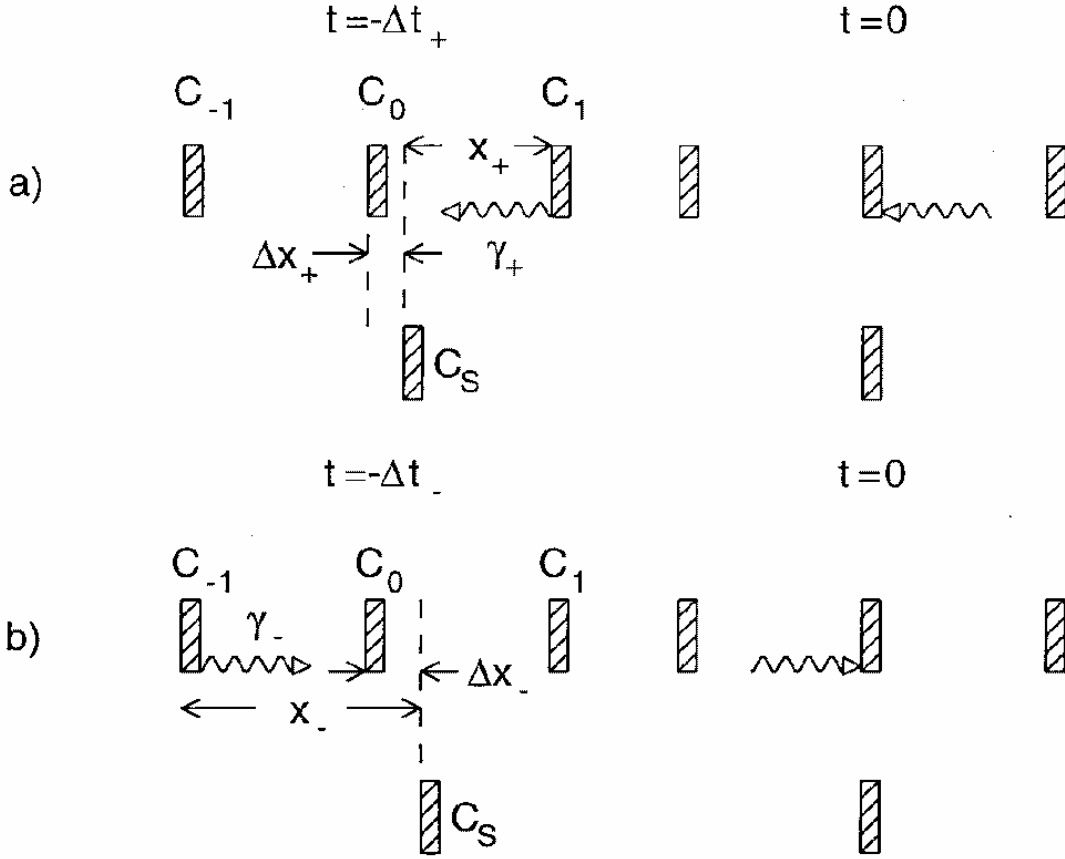


Figure 11: Propagation time delay effects. In a) the photon γ_+ emitted by C_1 at time $t = -\Delta t_+$ arrives at the observer beside C_S at $t = 0$. Thus $\Delta t_+ = x_+/c = \Delta x_+/v$. In b) the photon γ_- emitted by C_{-1} at time $t = -\Delta t_-$ also arrives at C_S at $t = 0$. and $\Delta t_- = x_-/c = \Delta x_-/v$. In a), [b)] the observed clock is receding from [approaching] the observer. Since evidently $x_- > x_+$ it follows that $\Delta t_- > \Delta t_+$ so that the effects of LPTD are larger for approaching than for receding clocks. A corollary (see Ref[5]) is that at $t = 0$ the clock C_{-1} appears more distant than the clock C_1 .

so that

$$t'_{m,j+1} - t'_{m,j} = \sqrt{\frac{1-\beta}{1+\beta}} \tau \quad (x_m > 0) \quad (4.29)$$

$$t'_{m,j+1} - t'_{m,j} = \sqrt{\frac{1+\beta}{1-\beta}} \tau \quad (x_m < 0) \quad (4.30)$$

Comparing Eqns(4.29),(4.30) with (4.20) it can be seen that, when the LPTD are taken into account the TD formula for a local clock is replaced by the Relativistic Doppler Effect formulae Eqns(4.29),(4.30). Actually, for $x_m < 0$ the clock appears to run fast, not slow. Just, as pointed out in Refs.[2,3,4], a moving sphere does not appear flattened by the LFC effect, Eqns.(4.29) and (4.30) demonstrate that a moving local clock does not show the TD effect. Weinstein [5] considered length measurements (for example the distance between successive clocks on the train in the present example) under the same conditions as the time measurements described by Eqns.(4.29), (4.30) where a single observer is close to a moving object. If l_0, l denote the lengths of an object viewed in S', S then the relation between l_0 and l is given by the replacements $\tau \rightarrow l_0, \Delta t' = l$ in Eqns.(4.29),(4.30). Thus an approaching clock (apparently running fast) appears more distant than a receding clock which is apparently running slow. Neither the LFC nor the TD effects are directly observed when LPTD are taken into account.

It is interesting to note the identity of Eqns.(4.29),(4.30) with the usual Relativistic Doppler Shift formulae which, following Ref.[1] are usually derived by considering the LT properties of Electromagnetic Waves. Here they have been derived from considerations of space-time geometry, as applied to events corresponding to the emission or absorption of photons. No use is made of the wave concept.

Writing Eqns.(4.27),(4.28) in terms of (n, j) gives the equations:

$$t'_{n,j} = \gamma[j - \beta n]\tau \quad (n > 0) \quad (4.31)$$

$$t'_{n,j} = \gamma[j + \beta n]\tau \quad (n < 0) \quad (4.32)$$

Both Eqns.(4.31) and (4.32) yield the result:

$$t'_{n,j+1} - t'_{n,j} = \gamma\tau \quad (4.33)$$

Thus the TC effect of Eqn(4.23) is unchanged by LPTD corrections (they must clearly be the same at fixed n or x). The apparent time delay between the clocks on successive wagons is, including the effect of LPTD :

$$t'_{n+1,j} - t'_{n,j} = -\gamma\beta\tau \quad (n > 0) \quad (4.34)$$

$$t'_{n+1,j} - t'_{n,j} = \gamma\beta\tau \quad (n < 0) \quad (4.35)$$

Comparing with Eqn.(4.24) it can be seen that the LPTD increases the absolute size of the delay and, for $n < 0$ (EC approaching the observer) changes the sign of the effect.

The effect of LPTD corrections on the clock C_m may be calculated by taking the difference between $t'_{m,j}$ given by Eqn.(4.27) or (4.28) and $t'_{m,j}$ given by Eqn.(4.19). The

results are:

$$\Delta'_{j,m} \equiv t'^D_{m,j} - t'_{m,j} = \frac{[\gamma^2(1-\beta) - 1]}{\gamma} [m + j] \quad (x_m > 0) \quad (4.36)$$

$$\Delta'_{j,m} \equiv t'^D_{m,j} - t'_{m,j} = \frac{[\gamma^2(1+\beta) - 1]}{\gamma} [m + j] \quad (x_m < 0) \quad (4.37)$$

The apparent times shown by the EC at $t = 0$, $t = \tau$, taking into account LPTD are presented in Table 6 and shown, for the special case $\beta = 0.6$ in Fig 12. Included also in Table 6 and Fig 12 is the ‘Magic Clock’ \overline{C}_M situated at $x' = x'_M$ where :

$$x'_M = -\frac{L}{\gamma\beta} \left[1 - \sqrt{\frac{1-\beta}{1+\beta}} \right] \quad (4.38)$$

which indicates the same time as C_S at $t = \tau$. Table 6 and Fig.12 show the perhaps surprising result that the EC situated symmetrically in x relative to C_S at time $t = 0$ and $t = \tau$ apparently lag C_S by identical times. This is because the time asymmetry between positive and negative x produced by the LT (see Fig.10) is exactly compensated by the LPTD. For example. at $t = \tau$ the LT gives the result for $\beta = 0.6$ that C_0 lags C_S by 0.2τ . However, the longer time delay from C_{-2} as compared to C_0 (see Fig.11) means that after correcting for LPTD, C_{-2} appears also to lag C_S , by just the same amount as C_0 , which has a smaller LPTD correction.

Finally in this section the region of the space-time domain of S' , that is visible to the observer in S is discussed. In particular the space-time observations which may be made of the wagon holding the EC C_0 during the period $0 < t < \tau$ when it is passing by the Standard Clock C_S will be considered. The situation is shown for the three cases: $\beta = 0.0, 0.6, 0.943$ ($\gamma = 1.0, 1.25, 3.0$) in Figs 13a),b),c) respectively. For $\beta = 0$ the history of each part of the wagon may be observed in an unbiased manner over the whole period. When the wagon is moving as in Fig 9b), late times at the front and early times at the rear of the wagon are no longer observable. The observable region of the (x', ct') plane is only that between the lines L1, L2 (Fig 13b)) where:

$$L1 : ct' = -\beta x' \quad (4.39)$$

$$L2 : ct' = -\beta x' + \frac{c\tau}{\gamma} \quad (4.40)$$

As β approaches one (Fig 13c) the observable domain occupies only a narrow region around the backward light cone of the origin of S' . So, although the wagons of the train are more concentrated in the field of vision of an observer in S , due to the LFC, the fraction of the total space-time area of S' that may be observed becomes vanishingly small. Note that the boundaries of the observable area in the space-time of S' are easily read off from the apparent time of the clocks C_{-1}, C_0 recorded in Table 5. Eqns.(4.39) and (4.40) are derived from Eqn.(4.19) with $j = 0, 1$ respectively on making the replacements: $\tau \rightarrow L/\gamma v$, $m \rightarrow x'/L$. The situation shown in Fig 13 Corresponds to the observation of the train at a distance such that the angle subtended by the wagon between C_0 and C_{-1} at the observer is small. In this case the effects of LPTD essentially cancel. It is

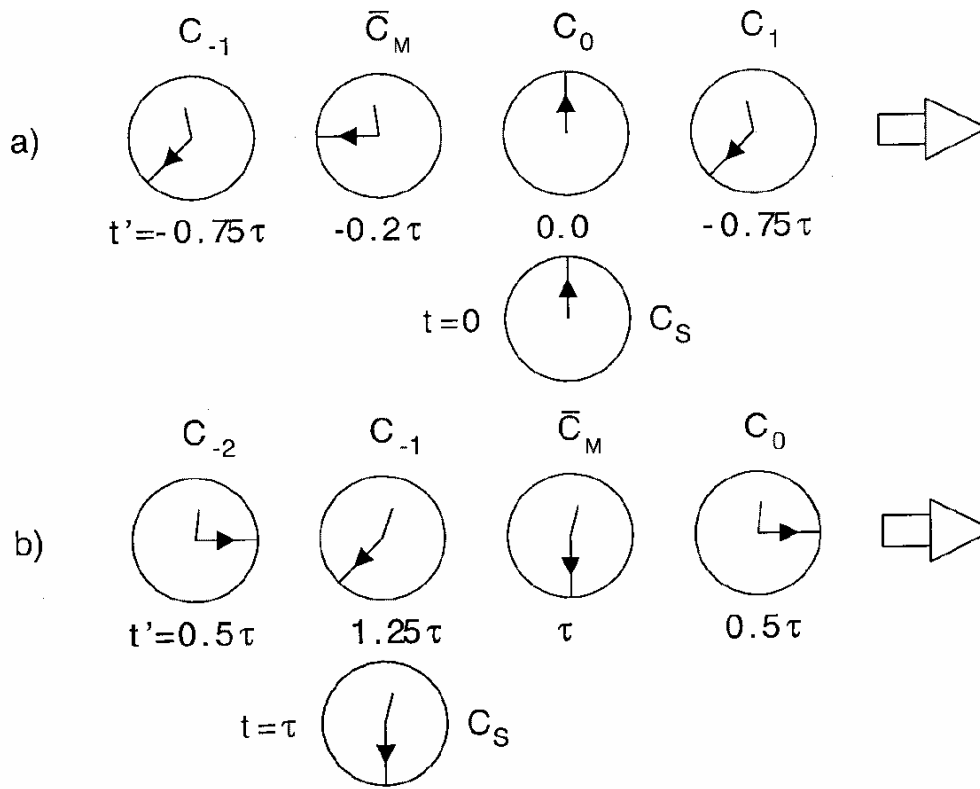


Figure 12: As Fig.10, but including the effects of LPTD.

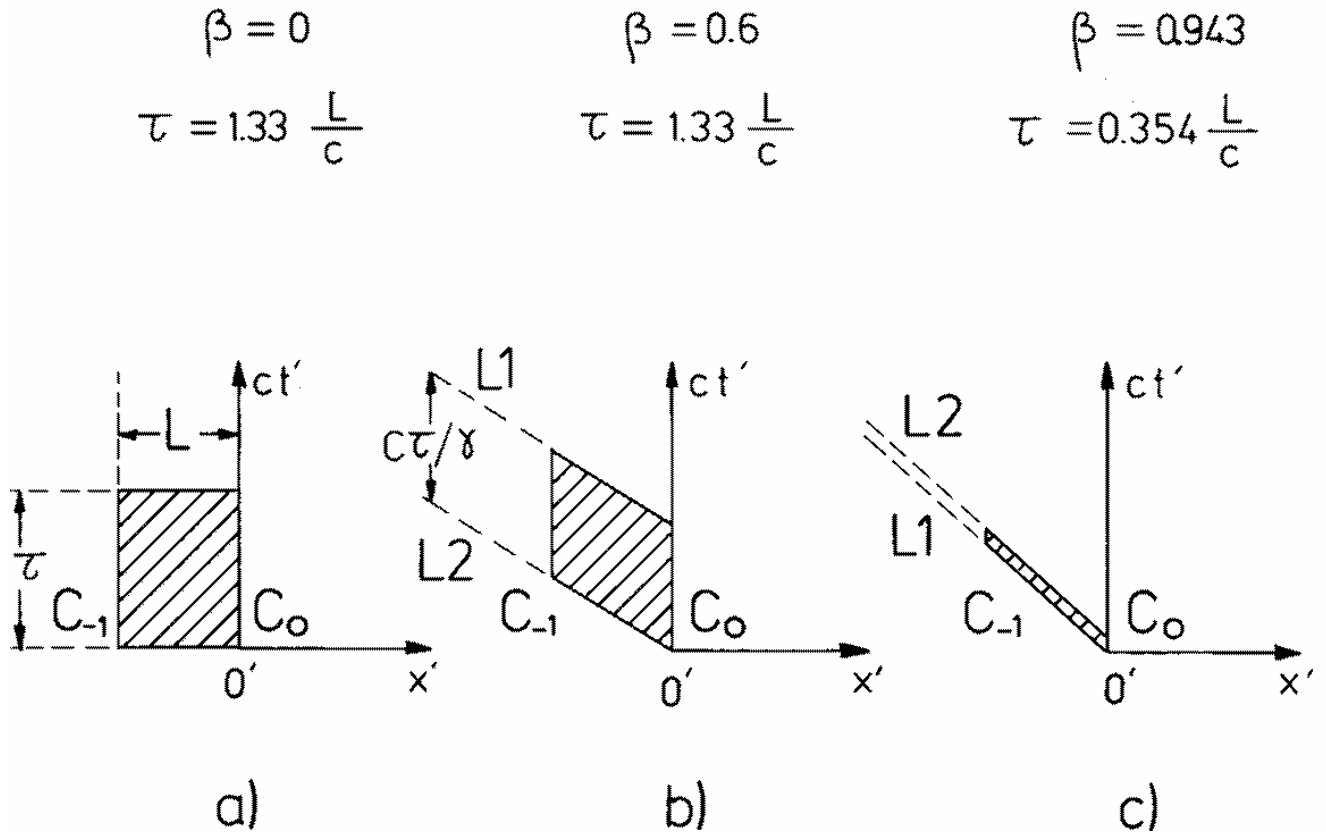


Figure 13: The domains of (x', ct') space (cross-hatched) of the wagon holding the clock C_0 (see Fig.9) seen by an observer in S' during the time $0 < t < \tau$. a),b),c) are for $\beta = 0, 0.6, 0.943$ respectively. Without effects of LPTD, as in the case of an observer at a large transverse distance from the train.

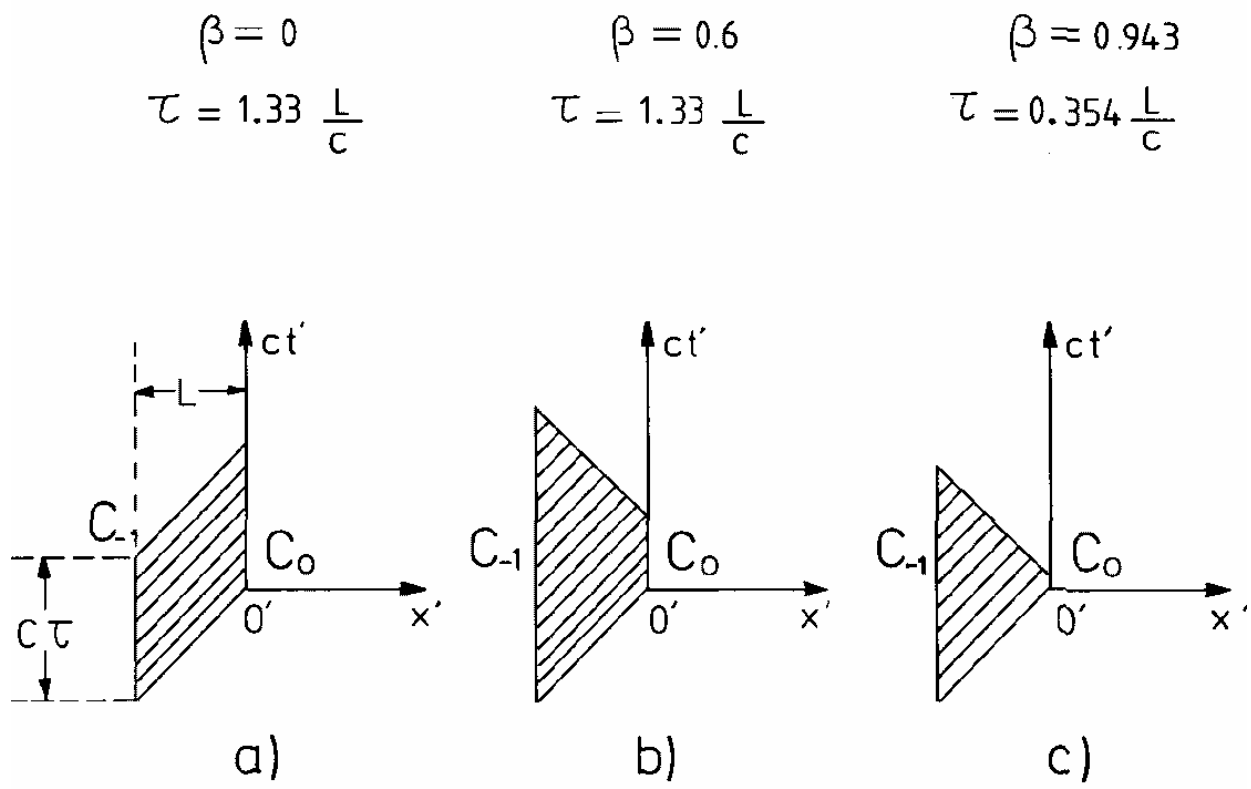


Figure 14: As Fig.13, for an observer close to the train, and including the effects of LPTD.

interesting to compare this with the case of an observer close to the train when the LPTD of photons moving almost parallel to the train must be taken into account. The (x', ct') domain seen by such an observer, for the same conditions as in Fig 13, is shown in Fig 14. It is derived in a similar way as for Fig.13, starting from Eqn.(4.28) instead of Eqn.(4.19). When the train is moving the observable range of t' is always greater at the rear end (position of C_{-1}) than at the front (position of C_0) of the wagon. As $\beta \rightarrow 1$ the t' range at C_0 vanishes and that at C_{-1} approaches a constant $-L/c < t' < L/c$, corresponding to the full region between the forward light cone ($x' = ct'$) and the backward light cone ($x' = -ct'$) of the origin of S' .

5 Discussion

The different space-time effects (apparent distortions of space or time) in Special Relativity that have been discussed above are summarised in Table 7. These are the well-known LFC and TD effects, Space Dilatation (SD) introduced in Section 3 above, and Time Contraction (TC) introduced in Section 4. Each effect is an observed difference Δq ($q = x, x', t, t'$) of two space or time coordinates ($\Delta q = q_1 - q_2$) and corresponds to a constant projection $\Delta \tilde{q} = 0$ ($\tilde{q} \neq q$) in another of the four variables x, x', t, t' of the LT. As shown in Table 7, the LFC, SD, TC and TD effects correspond, respectively, to the Δt , $\Delta t'$, Δx and $\Delta x'$ projections. After making this projection, the four LT equations give two relations among the remaining three variables. One of these describes the ‘space-time distortion’ relating $\Delta t'$ and Δt or $\Delta x'$ and Δx while the other gives the equation shown in the last column, (labelled ‘Complementary Effect’) in Table 7. These equations relate either Δx to Δt (for SD and TD) or $\Delta x'$ to $\Delta t'$ (for LFC and TC). It can be seen from the Complementary Effect relations that the two space-time points defining the effect (of space-time distortion) are space-like separated for LFC and SD and time-like separated for TC and TD.

For example, for the LFC when $t_1 = t_2 = t$, the LT equations for the two space-time points are:

$$x'_1 = \gamma(x_1 - vt) \quad (5.1)$$

$$x'_2 = \gamma(x_2 - vt) \quad (5.2)$$

$$t'_1 = \gamma\left(t - \frac{\beta x_1}{c}\right) \quad (5.3)$$

$$t'_2 = \gamma\left(t - \frac{\beta x_2}{c}\right) \quad (5.4)$$

Subtracting (5.1) from (5.2) and (5.3) from (5.4) gives:

$$\Delta x' = \gamma \Delta x \quad (5.5)$$

$$\Delta t' = -\frac{\gamma\beta}{c} \Delta x \quad (5.6)$$

Name	Observed Quantity	Projection	Effect	Complementary Effect
Lorentz-Fitzgerald Contraction (LFC)	Δx	$\Delta t = 0$	$\Delta x = \frac{1}{\gamma} \Delta x'$	$\Delta x' = -\frac{c}{\beta} \Delta t'$
Space Dilatation (SD)	Δx	$\Delta t' = 0$	$\Delta x = \gamma \Delta x'$	$\Delta x = \frac{c}{\beta} \Delta t$
Time Contraction (TC)	$\Delta t'$	$\Delta x = 0$	$\Delta t' = \gamma \Delta t$	$\Delta x' = -c\beta \Delta t'$
Time Dilatation (TD)	$\Delta t'$	$\Delta x' = 0$	$\Delta t' = \frac{1}{\gamma} \Delta t$	$\Delta x = c\beta \Delta t$

Table 8: The different apparent distortions of space-time in Special Relativity (see text).

Eqn.(5.5) describes the LFC effect, while combining Eqns.(5.5) and (5.6) to eliminate Δx yields the equation for the Complementary Effect. By taking other projections the other entries of Table 7 may be calculated in a similar fashion. It is interesting to note that the TD effect can be derived directly from the LFC effect by using the symmetry of the LT equations. Introducing the notation: $s \equiv ct$, the LT may be written as:

$$x' = \gamma(x - \beta s) \quad (5.7)$$

$$s' = \gamma(s - \beta x) \quad (5.8)$$

These equations are invariant ⁵ under the following transformations:

$$T1 : x \leftrightarrow s, \quad x' \leftrightarrow s' \quad (5.9)$$

$$T2 : x \leftrightarrow x', \quad s \leftrightarrow s', \quad \beta \rightarrow -\beta \quad (5.10)$$

Writing out the LFC entries in the first row of Table 7, replacing t, t' by $s/c, s'/c$; gives

$$\Delta x \quad \Delta s = 0 \quad \Delta x = \frac{\Delta x'}{\gamma} \quad \Delta x' = -\frac{\Delta s'}{\beta}$$

Applying $T1$ to each entry in this row results in:

$$\Delta s \quad \Delta x = 0 \quad \Delta s = \frac{\Delta s'}{\gamma} \quad \Delta s' = -\frac{\Delta x'}{\beta}$$

Applying $T2$:

$$\Delta s' \quad \Delta x' = 0 \quad \Delta s' = \frac{\Delta s}{\gamma} \quad \Delta s = \frac{\Delta x}{\beta}$$

Replacing $\Delta s, \Delta s'$ by $c\Delta t, c\Delta t'$ yields the last row of Table 7 which describes the TD effect. Similarly TC can be derived from SD (or vice versa) by successively applying the transformations $T1, T2$.

A remark on the ‘Observed Quantities’ in Table 7. For the LFC, SD the observed quantity is a length interval in the frame S. The apparent space distortion occurs because this length differs from the result of a similar measurement made on the same object in its own rest frame. $\Delta x'$ is not directly measured at the time of observation of the LFC or

⁵ Actually the transformation $T2$ yields the inverse of the LT (5.7),(5.8). The inverse equations may then be solved to recover (5.7) and (5.8)

SD. It is otherwise with the time measurements TD, TC. Here the time interval *in their own rest frame* indicated by a moving clock (TD), or different equivalent clocks at the same position in S (TC), is supposed to be directly observed and compared with the time interval Δt registered by an unmoving clock in the observer's rest frame. Thus the effect refers to two simultaneous observations by *the same observer* not to separate observations by *two different observers* as in the case of the LFC and SD.

Einstein's great achievement in his first paper on Special Relativity [1] was, for the first time, to clearly disentangle in Classical Electromagnetism, the purely geometrical and kinematical effects embodied in the Lorentz Transformation from dynamics. In spite of this, papers still appear from time to time in the literature claiming that moving objects 'really' contract [6] or that moving clocks 'really' run slow [7] for dynamical reasons, or even that such dynamical effects are the true basis of Special Relativity and should be taught as such [8]. As it has been shown above that a moving object can apparently shrink or expand, and identical moving clocks can apparently run fast or slow, depending only on how they are observed, it is clear that they cannot 'really' shrink, or run slow, respectively. If a moving object actually shrinks for dynamical reasons it is hard to see how the same object, viewed in a different way (in fact only illuminated differently in its own rest frame) can be seen to expand. Certainly both effects cannot be dynamically explained. In fact the Lorentz Transformation, as applied to space-time, describes only the *appearance* of space-time events, a purely geometrical property. The apparent distortions are of geometrical origin, the space-time analogues of the apparent distortions of objects in space, described by the laws of perspective, when they are linearly projected into a two dimensional sub-space by a camera or the human eye.

In conclusion the essential characteristics of the two 'new' space-time distortions discussed above are summarised :

- Space Dilatation (SD): If a luminous object, lying along the Ox' axis at rest in the frame S' , has a short luminous lifetime in this frame, it will be observed from a frame S , in uniform motion relative to S' parallel to Ox' at the velocity $-\beta c$, as a narrow line, perpendicular to the x -axis, moving with the velocity c/β in the same direction as the moving object. The total distance swept out along the x -axis by the moving line during the time $\beta l_0/(c\sqrt{1-\beta^2})$, for which the moving line image exists, is $l_0/\sqrt{1-\beta^2}$ where l_0 is the length of the object as observed in S' . Thus the apparent length of the object when viewed with a time resolution much larger than $\beta l_0/(c\sqrt{1-\beta^2})$ is $l_0/\sqrt{1-\beta^2}$. Any effects of LPTD are not taken into account.
- Time Contraction (TC): The equivalent clocks in the moving frame S' , viewed at the same position in the stationary frame S , apparently run faster by a factor $1/\sqrt{1-\beta^2}$ relative to a clock at rest in S .

Acknowledgements

I thank G.Barbier and C.Laignel for their valuable help in the preparation of the figures.

References

- [1] A.Einstein, 'Zur Elektrodynamik bewegter Körper', Annalen der Physik **17** (1905), 891.
- [2] J.Terrell, 'Invisibility of the Lorentz Contraction' Phys. Rev. **116** (1959), 1041-1045.
- [3] R.Penrose, Proc. Cambridge Phil. Soc. **55** (1959), 137.
- [4] V.F.Weisskopf, 'The Visual Appearance of Rapidly Moving Objects', Physics Today, Sept. 1960 pp24-27.
- [5] R.Weinstein, 'Observation of Length by a Single Observer', Am. J. Phys. **28** (1960), 607-610.
- [6] R.A.Sorenson, 'Lorentz contraction, a real change of shape', Am. J. Phys. **63** (1995), 413-415.
- [7] O.D.Jefimenko, 'Direct calculation of time dilation', Am. J. Phys. **64** (1996), 812-814.
- [8] J.S.Bell, 'How to teach special relativity', in 'Speakable and Unspeakable in Quantum Mechanics', Cambridge University Press, (1987), pp67-80.